European Journal of Wood and Wood Products (2024) 82:1021–1035
https://doi.org/10.1007/s00107-024-02074-2

ORIGINAL ARTICLE

Tropical mobola plum (*Parinari Curatellifolia*): a full characterization of wood and bark within the scope of biorefineries

Abílio Malengue[1,2] · Ana Lourenço[1] · Helena Patrício[1] · Ricardo A. Costa[1] · Teresa Quilhó[1] · Jorge Gominho[1]

Received: 23 October 2023 / Accepted: 28 March 2024 / Published online: 8 April 2024
© The Author(s) 2024

Abstract

Parinari curatellifolia is the main species used to produce charcoal in Angola. Its chemical, anatomical, and thermal properties were analyzed. The bark is dark grey, rough, and corky, and the wood is brown to yellow-red. Compared to wood, bark fibers presented lower length, lumen, and wall thickness. There is not much difference between height and cell numbers of rays. Sieve tube elements appear solitary or in small groups (2–3 cells), and vessels were of two diameter classes but diffuse-porous. Bark basic density was lower than wood (505 kg.m^{-3}vs. 580 kg.m^{-3}). The mean chemical composition from bark vs. wood of *P. curatellifolia* was ash (3.2% vs. 1.6%), total extractives (12.2% vs. 10.0%), total lignin (42.4% vs. 28.4%), and suberin 5.4%. Families identified by GC-MS from DCM extracts were predominated by fatty acids in wood and triterpenoid contents in bark. Bark and wood had higher antioxidant activity in FRAP and DPPH methods. The bark had a monomeric lignin composition richer in guaiacyl-units (25.9% vs. 22.5%) and lower syringyl-units (5.7% vs. 8.5%). Potassium was the most abundant mineral, while the least was cadmium found in wood and bark. Regarding thermal properties, bark presented higher moisture content (9.0% vs. 8.0%), ash (3.33% vs. 1.61%), total volatiles (27.5% vs. 20.7%), lower fixed carbon (69.1% vs. 77.7%) and higher heating value (20.9 MJ/kg vs. 19.1 MJ/kg). According to these characteristics, both biomasses are interesting for developing more value-added products (e.g., charcoal, bio-chemicals with phytochemistry and pharmacology activities) besides burning under the context of biorefineries.

1 Introduction

The mobola plum, scientifically known as *Parinari curatellifolia* (Planch. ex Benth.), is also called uchia, mendonça, muchacha, cork tree, grysappel, loxa, uyengyo, and olonsha (Maharaj and Glen 2008; Orwa et al. 2009; Sanfilippo 2014). This tree belongs to the *Chrysobalanaceae* family, previously classified under the *Rosaceae* order due to its physical characteristics (Carnevale Neto et al. 2013). It is a medium to large evergreen tree that can grow up to 20 m tall, with a bare stem and a dense, roundish mushroom-shaped crown (Orwa et al. 2009). This species is widely distributed in Angola and the central region of Africa (Palgrave 2002; Sanfilippo 2014). *P. curatellifolia* is an indigenous fruit species, an important food source for many rural communities (Shoko et al. 2014), and one of the most important medicinal plants (Mawire et al. 2021). For this reason, studies on the bark are mostly related to its evaluation for phytochemistry and pharmacology (Carnevale Neto et al. 2013; Halilu et al. 2013; Omale et al. 2020). Uses in ethnomedicine included treating wound infections, cancer, pneumonia, fever, bacterial infections, and inflammation disorders (Gororo et al. 2016; Kundishora et al. 2020). The plant also has other different uses, i.e., the bark and leaf extracts can be used for tanning, and bark produces a pink-brown dye which is generally used in basket work (Maharaj and Glen 2008); seed oil content is suitable for biodiesel production (Nabora et

✉ Jorge Gominho
jgominho@isa.ulisboa.pt

[1] Centro de Estudos Florestais, Laboratório Associado TERRA, Instituto Superior de Agronomia, Universidade de Lisboa, Tapada da Ajuda, Lisboa 1349-017, Portugal

[2] Faculdade de Ciências Agrárias da Universidade José Eduardo dos Santos, Huambo, Angola

al. 2019). The wood is very durable, hard, and heavy and is used as charcoal or for firewood purposes (Bolza and Keating 1972); despite its high silica content, which is problematic because it blunts the blades of saws and other tools (Sanfilippo 2014), wood is often used for woodwork, mortars, manufacture of pounding blocks or poles (Maharaj and Glen 2008; Orwa et al. 2009), as well as boats due to their resistance to marine borers (Bolza and Keating 1972; Flora Malesiana 1989; Prance 2007).

Despite the importance of this species, studies on its bark and wood anatomy are scarce, and few or no detailed descriptions were found. In addition, it is known that structural and anatomical features highly influence the wood's performance as a material. To our knowledge, this is the first detailed report on the bark anatomy of *P. curatellifolia*, although a recent study on cellular and chemical features of its cork was published (Malengue et al. 2023). Metcalfe and Chalk (1950) gave some information on the general bark anatomy of various genus of *Chrysobalanaceae*, including species of *Parinari*, and Roth (1981) characterized the bark structure of some genus of the group with a focus on the anatomy of species belonging to the genus *Licania* and only occasionally gave remarks of *P. excelsa* and *P. rodolphii*. Wood anatomy of *Chrysobalanaceae* was described in Flora Malesiana (1989) and InsideWood (2004), but reports on wood anatomical characterization of *P. curatellifolia* are limited and set up with other species of the genus. In Richter and Dallwitz (2000) various genus of *Parinari* were described, however, without any references for *P. curatellifolia*. In a recent study, Massuque et al. (2021b) evaluated the effect of fiber and vessel biometry on wood combustibility.

Charcoal production, like deforestation and forest degradation, causes a sizeable environmental impact and is continuously growing in African rural communities (Miapia et al. 2021). Thus, more knowledge is needed on the chemical properties of miombo wood species, emphasizing those less used for the wood industry and exploited for charcoal and firewood production (Lhate et al. 2010). This research seeks to provide a detailed description of the bark and wood anatomy of *P. curatellifolia*, including a comparison with other *Chrysobalanaceae* species. The study also examines the chemical composition of the wood and bark, including ash, extractives, suberin, lignin, and holocellulose. Furthermore, the research evaluates the monomeric lignin composition, lipophilic extracts composition, phytochemical profile, and antioxidant activities of ethanol and water extracts. This is the first time such comprehensive data has been gathered on *P. curatellifolia* that may contribute to its expansion management and use along with the traditional applications but more efficiently, keeping in mind the scope of biorefineries and the implementation of Sustainable Development Goals of the United Nations (1, 2, 3, and 7).

2 Materials and methods

2.1 Site characterization and sampling

Three trees of *P. curatellifolia* were collected at Cuima, the municipality of Caala, located in Huambo, Angola (13° 33.216'S and 15°36.956'E). The region is 1700 m a.s.l. (above sea level), it has a mean annual temperature of 20 °C and rainfall that ranges from 1200 to 1600 mm per annum. The dominant soils are ferrosols, usually found at higher elevations, followed by fluvisols, which are more common at lower elevations (Chiteculo et al. 2022), with a pH from 5.5 to 6.5 and low nutrient content (Delgado-Matas and Pukkala 2015). The annual relative humidity varies from 60 to 70% (Ndjamba et al. 2021). The mean tree total height and diameter at breast height (DBH) were respectively 8.5 m (± 1.7) and 14.8 cm (± 1.2); stem sectional discs of 3–4 cm thickness were taken from each tree at DBH.

2.2 General features

For observation and measurement, the transverse surfaces of the discs were polished with sandpaper, and two cross diameters were measured for bark thickness determination. Samples were observed with a handheld digital microscope Dino-Lite AM4113ZT.

2.2.1 Anatomical characterization

Bark samples were impregnated with polyethylene glycol (DP1500). Transverse and longitudinal microscopic sections of approximately 17 µm thickness were prepared with a Leica SM 2400 microtome using Masking Tape 3 M 101E, according to Barbosa et al. (2010). The sections were stained with a double chrysoidine-astra blue staining and mounted on Kaiser Glycerin. After 24 h, the lamellas were submerged into xylol for 30 min to remove the adhesive, dehydrated in 96% and 100% ethanol, and mounted in Eukitt. Sudan 4 was used for selective staining of suberin. The bark samples were also observed by scanning electronic microscopy (SEM) with a TM3030Plus Tabletop Microscope (Hitachi) with different magnifications, and the images were recorded in digital format.

Wood samples were cut from the mature wood and softened in boiling water. Transverse and longitudinal sections approximately 17 µm thick were prepared with a sliding microtome, stained with safranin, and mounted in Eukitt.

Additionally, bark and wood samples were macerated in a 1:1 solution of 30% H_2O_2 and CH_3COOH at 60 °C for 48 h and stained with astra blue (Franklin 1945). The length, width, and cell wall thickness of 40 fibers (bark/wood) and the length and tangential diameter of 25 sieve tube members and vessel elements per individual were determined. All measurements were done according to IAWA (1989) and Angyalossy et al. (2016) recommendations for wood and bark and Leica Qwin software was used. Analysis of variance (ANOVA) was applied to evaluate significant differences between trees for the anatomical variables of bark and wood. Differences were assessed with Duncan's post hoc tests. Statistical significance was set at $p < 0.05$. SigmaPlot® (Version 11.0, Systat Software, Inc., Chicago, IL, USA) was used for all statistical analyses.

Light microscopy observations were made using Leica DM LA, and photomicrographs were taken with a Nikon Microphot-FXA. The terminology used for the bark was followed by Junikka (1994) and Angyalossy et al. (2016), and for the wood, IAWA (1989).

2.2.2 Bark and wood density

The basic density of bark and wood was calculated using water displacement for green volume determination and oven-dry weight according to TAPPI 258 om-2 (TAPPI 2002a).

2.2.3 Chemical summative analysis

The 40–60 mesh size fraction of the wood and bark from *P. curatellifolia* included the determination of ash, extractives, suberin, acid-insoluble lignin (Klason), and acid-soluble lignin and the monomeric composition of polysaccharides following the methodology described by Neiva et al. (2018), Vangeel et al. (2021), and Gominho et al. (2021). Ash content was determined by combusting approximately 1.5 g of the sample overnight at 525 °C and weighing the residue, following TAPPI standard T211 om-93 (TAPPI 2007a). Extractives were determined using extraction thimbles by successive Soxhlet extractions with dichloromethane (DCM, 6 h), ethanol (16 h), and water (16 h) as mass loss of the oven-dried thimbles after each extraction. Suberin content was performed in the extractive-free material using methanolysis to depolymerize 1.5 g extractive-free bark as described in Malengue et al. (2023).

The Klason lignin and soluble lignin in the extractive-free material were measured using TAPPI standards T222 om-88 (TAPPI 2002b)and UM250 om-83 (TAPPI 1991), respectively. The ash content of the Klason lignin was considered when making the necessary adjustments. The monosaccharide composition of the polysaccharide fractions was determined in the hydrolysis liquor resulting from the acid-insoluble lignin. The neutral monosaccharides and galacturonic acid were separated by high-pressure ion-exchange chromatography in a Dionex ICS3000 equipped with a PAD detector using a Carbopac PA10 (4 × 250 mm) column plus Aminotrap and the eluent was $NaOH + CH_3COONa$ with a flow of 1 mL/min at 25 °C. Acetic acid was separated in a Waters 600 and measured with a UV/Vis detector at 210 nm, with a Biorad Aminex 87 H HPX column (300 × 7.8 mm), and the eluent was 10 mN H_2SO_4 with a flow of 0.6mL/min at 30 °C. All the chemical analyses were made in triplicate.

2.2.4 GC-MS analysis

The dichloromethane extracts (DCM) obtained by Soxhlet extraction according to T204 Cm-97 (TAPPI 2007b), were dried in aliquots under nitrogen and then in a vacuum oven with phosphorus pentoxide. 1 mg of the extract was dissolved in 120 µL of pyridine and trimethylsilylated with 80 µL of bis(trimethylsilyl)trifluoroacetamide (BSTFA) and oven heated at 60 °C for 30 min. The derivatized dichloromethane extracts were injected in an Agilent GC 7890 A coupled to 5975 C MSD with the following parameters: oven temperature program ranging from 50 to 380 °C at varying rates; the volatiles were separated in a capillary column Zebron 7HG-G015-02 (Phenomenex, USA) with 30 m x 0.25 mm ID x 0.1 µm (film thickness) at a flow constant rate of He (1 mL/min); the injector temperature was 380 °C. The mass spectra of the compounds were compared to a GC-MS spectral library (Wiley, NIST, and personal library) to identify them as TMS derivatives. Semi-quantitative analysis was performed by expressing the relative proportions of the peaks in the total ion chromatograms as percentages.

2.2.5 Phytochemical profile and antioxidant activities

The extracts were obtained following the methodology described by Miranda et al. (2016). Approximately 0.250 g of the sample from the wood and bark of *P. curatellifolia* were extracted with ethanol/water (80:20 v/v) for 1 h at 40 °C using an ultrasonic bath, with a solid-liquid ratio 1:10 (m/v). The extract resulting from the filtration of the sample was used to evaluate the phytochemical profile: total phenolics (TPC, expressed as mg gallic acid equivalents (GAE)/g Extract), flavonoids (FC), condensed tannins (CTC) contents both expressed as catechin equivalents (CE)/g extract; all as through calibration curves (Neiva et al. 2018).

The antioxidant activity was attained following two methodologies described by Sánchez-Moreno et al. (1998): (i) FRAP (Ferric-reducing antioxidant power expressed (mM TEAC/g extract) and (ii) DPPH (free radical scavenging activity of 2,2-diphenyl-1-picrylhydrazyl). The

DPPH results were expressed as IC50 (extract concentration required for 50% DPPH inhibition), in terms of Trolox equivalents (TEAC) on a dry extract base (mg Trolox/mg extract) and as antioxidant activity index (AAI = final concentration of DPPH in the control sample/IC50). The AAI considers the mass of DPPH and test sample, decreasing the concentration influence of the DPPH solution used. The antioxidant activity was classified as poor if AAI < 0.5, moderate if 0.5 < AAI < 1, strong if 1 < AAI < 2, and very strong when AAI > 2 (Neiva et al. 2018). All the analyses were also made in triplicate, and results were expressed as average with standard deviation.

2.2.6 Analytical pyrolysis

Extractives-free samples from wood and bark of *P. curatellifolia* were previously milled in a Retsch MM20 mixer ball mill for 10 min, and around 0.10 mg of the sample was weighed. Each sample was pyrolyzed at 550 °C (for 1 min) in a platinum coil Pyroprobe connected to a CDS 5150 valved interface linked to a gas chromatographer (Agilent 7890B) and with a mass detector (Agilent 5977B). The volatiles formed were separated in a fused-silica capillary column (ZB-1701: 60 m x 0.25 mm i.d. x 0.25 µm film thickness, (Phenomenex, USA). The chromatographic conditions used were described in Malengue et al. (2023). The compounds were identified by comparing their mass spectra with the Wiley, NIST2014 database and literature (Faix et al. 1990; Ralph et al. 1991). The total area of the chromatogram was obtained automatically, and the percentage area of each compound identified was calculated. Total carbohydrates derivatives (C) and total lignin derivatives (L) were summed, and then the relation between carbohydrates and lignin was calculated and presented as the C/L ratio. The monomeric composition was also determined as H:G:S relation.

2.2.7 Quantitative determination of mineral content

About 300 mg of dry matter was placed in digestion with aqua regia acid solution (a mixture of hydrochloric acid with nitric acid in the ratio of 3:1) for 90 min at 105 °C (Gaudino et al. 2007). The ICP-OES analytical technique (Inductively Coupled Plasma-Optical Emission Spectrometry) was applied to determine the elemental composition from wood and bark of *P. curatellifolia* using the Thermo Scientific TM iCAPTM 7400 ICP-OES analyzer (Thermo Fisher Scientific, Bremen, Germany).

2.2.8 Proximate analysis and ultimate analysis

Proximate analysis was performed using the ASTM E870-82 method (ASTM 2019). Ultimate analysis was determined following the ASTM standard method D5373-08(ASTM 2013) on an Elemental analyzer (Thermo Finnigan-CE Instruments Flash EA 1112 CHNS series). The oxygen content was obtained by subtracting from 100% the sum of (C, H, N, S, and ash) contents in percentage. Moisture content, ash content, total volatiles, and fixed carbon were determined following the methodology described by Costa et al. (2023).

2.2.9 Data analysis

Statistical analyses of anatomical features were performed using the software R version 4.3.0. for Windows. Significance was tested using a one-way ANOVA and comparing mean values via the Tukey post hoc test. The level of significance was always set to $p < 0.05$.

3 Results and discussion

3.1 General features

The bark of *P. curatellifolia* is dark grey, rough, and corky (Fig. 1a), and the wood is brown to yellow-red. The average bark thickness was 1.2 (±0.2) mm, including the rhytidome and the phloem. The phloem was 0.5 (±0.1) mm thick and comprised the conducting phloem distinct from the non-conducting phloem by different colors due to the amount of sclerenchyma tissue. Growth increments were detected in the rhytidome and observable by the naked eye (Fig. 1b).

3.2 Bark anatomical characterization

The general anatomy of *P. curatellifolia* bark had some similarities with another genus of the *Chrysobalanaceae* studied by Roth (1981), i.e., in some *Licania* sp. concerning the abundance of mechanical tissue, especially in the form of the nodules of sclereids, fibro-sclereids and reduced fibers, type of rays and dilatation tissue.

The rhytidome is moderately developed, appearing as small scales (Fig. 1b); a structural pattern in the rhytidome is recognized with a variable number of undulated periderm layers (2–4) intercalated with phloemic tissue, which includes compact nodules of sclerified tissues (Fig. 1b-e); in the periderm produced by the phellogen, the phellem cells (typical cork cells, Fig. 1c-g) with thin walls are relatively abundant and arranged regularly in radial rows, some with brown cell contents alternating with others,

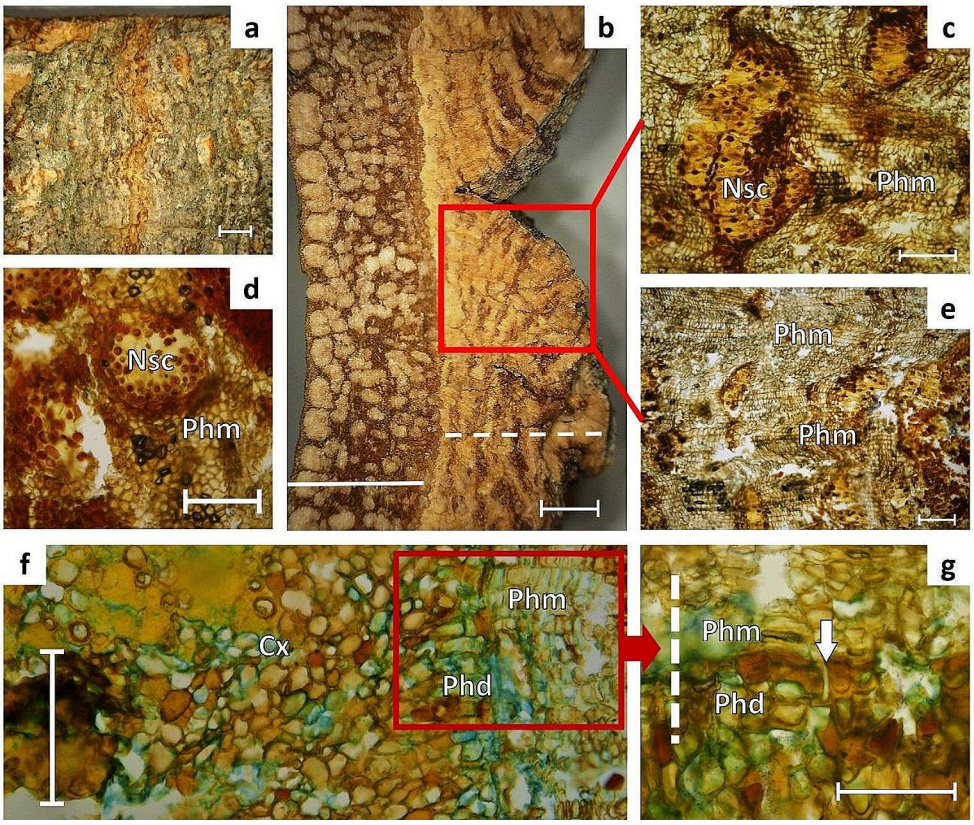


Fig. 1 Bark of *Parinari curatellifolia*: **a**) External aspect of rhytidome; **b**) Phloem (——) and rhytidome (---) in transverse section; **c-e**) rhytidome with nodules of sclereids (Nsc) and phellem cells (Phm) in tangential (**d**) and transverse sections (**c, e**); **f**) Cortical cells (Cx), phellem (Phm), and phelloderm (Phd) in radial section; **g**) portion periderm (-----) composed by the phellem cells (Phm), phellogen (arrow), and phelloderm (Phd) in transverse section. **a**, **b** bark observed under a digital microscope Dino-Lite and **c-g** under a light microscope. Scale bar: **a**, **b** = 2 mm; **c-e** = 200 µm; **f**, **g** = 100 µm

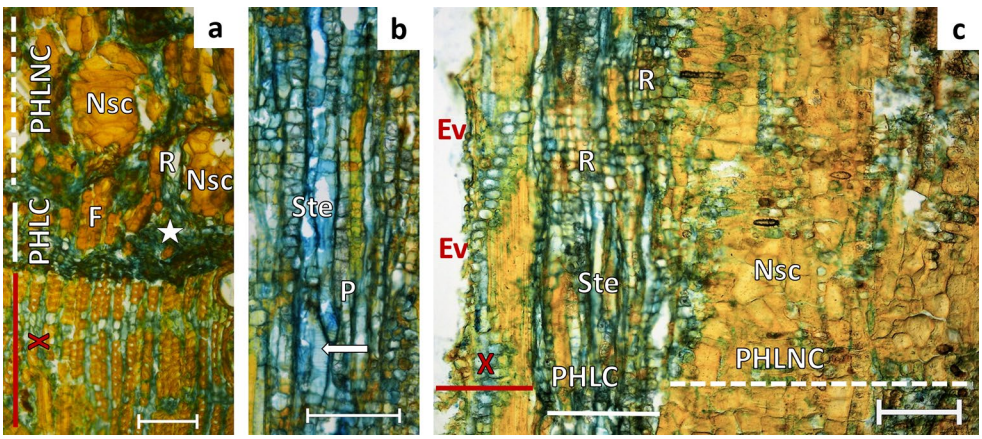


Fig. 2 Phloem and xylem of *Parinari curatellifolia*: **a**) Conducting phloem (PHLC) and nonconducting phloem (PHLNC), fibers (F), rays (R), nodules of sclereids (Nsc), and sieve tube elements mixed with axial parenchyma cells represented by the annotation and xylem (X), in transverse section. **b**) Portion of conducting phloem with sieve tube elements (Ste) with numerous sieve areas (arrow) and axial parenchyma cells (P) in tangential section; **c**) Conducting phloem (PHLC) and nonconducting phloem (PHLNC), sieve tube elements (Ste), rays (R), nodules of sclereids (Nsc) and vascular elements (Ev) of the xylem, in radial section. Scale bar: **a**, **c** = 200 µm, **b** = 150 µm

colorless and curving slightly, forming discontinuous arching layers in cross-section (Fig. 1c and e) and appearing somewhat radially stratified. The phelloderm is poorly developed, with 2–4 cells sometimes lignified with content and distinguished from cortical-like cells by their neat radial alignment (Fig. 1f-g); the observation of the phellogen is complex (Fig. 1g).

The phloem tissue produced by the vascular cambium is non-storied, comprised of the conducting and nonconducting phloem (Fig. 2a and c). The conducting phloem near the vascular cambium represents a tiny part of the phloem. It includes the sieve tube elements with companion cells (conducting cells), the axial parenchyma (storage tissue), rays (storage/transversal conduction), and the fibers (mechanical support) (Fig. 2a-b). The transition between conducting and

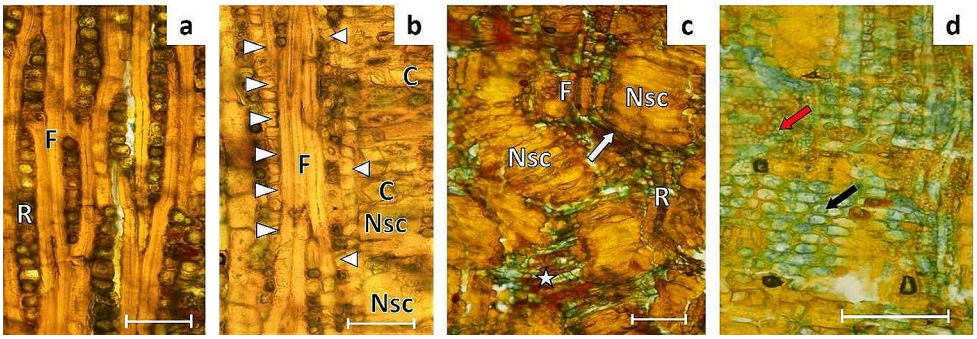


Fig. 3 Nonconducting phloem of *Parinari curatellifolia*: **a**) Rays mostly uniseriate (R) and radial parenchyma cells with thickened walls, thick-walled and pitted fibers (F); **b**) Strands of crystal-bearing axial parenchyma along the margins of the fiber (F) band (arrows), nodules of sclereids (Nsc) and crystals inside (C); **c**) Nodules of sclereids (Nsc) radially aligned, fibers (F), rays (R) and dilatation tissue (arrow) in transverse section; **d**) silica in cells of radial parenchyma (black arrow) and starch grains in axial parenchyma cells (red arrow); **a**, **b** (tangential sections); **c** (transverse section) and **d** (radial section). Scale bar: **a, b** = 100 µm, **c**, **d** = 200 µm

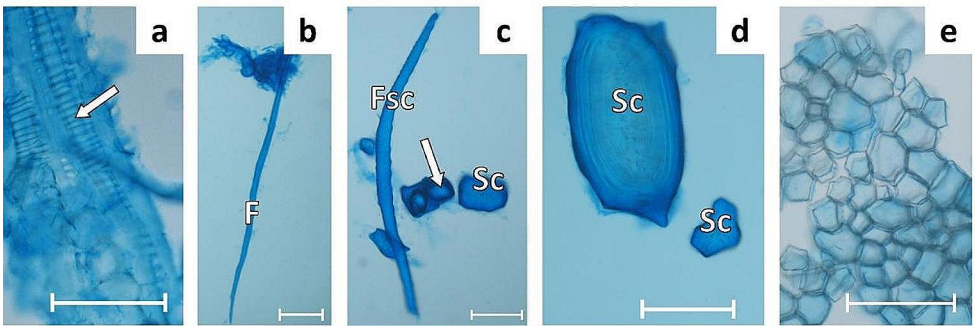


Fig. 4 Individualized cells of the bark of *Parinari curatellifolia*: **a**) Sieve plate (arrow) of the sieve tube elements; **b**) Fiber (F); **c**) Fiber-sclereids (Fsc), Sclereid (Sc) and crystals inside (arrow); **d**) Sclereids (Sc) with polylamellate walls; **e**) Phellem cells (cork cells). Scale bar: **a**, **c**, **d**, **e** = 100 µm, **b** = 150 µm

nonconducting tissue is somewhat abrupt, marked by the collapse of sieve tube elements and the formation of prominent nodules of sclerenchyma cells (Fig. 2a and c).

In the transverse view, the sieve tube elements appear round to polygonal with thin and unlignified cell walls dispersed between parenchyma cells and fibers, solitary or in small groups (2–3 cells); they can distinguish from neighboring parenchyma cells by their somewhat larger diameter. The sieve tube elements presented a mean length of 423 µm (± 17), ranging between 127 and 670 µm and a tangential diameter of 25 µm (± 9), ranging between 6 and 42 µm. The companion cells are difficult to recognize in transverse and longitudinal sections. Sieve plates are scalariform compound oblique, with > 10 areas per plate equally spaced (Fig. 2b).

In the conducting phloem, the axial parenchyma is relatively scarce in small layers near the sieve tube elements; parenchyma cells appeared rectangular or polygonal in the transverse section and have thin unlignified walls, but in nonconducting phloem cells could enlarge or radially divide giving rise to a dilatation tissue between the fibers and nodules of cluster sclereids; in the outer phloem beneath the recently formed periderm, a considerable amount of cells like cortical-cells appeared (Fig. 1f); strands of crystal-bearing axial parenchyma of up to 10 cells were found along the margins of the fiber band (Fig. 3b) near the nodules of sclereids. These crystalliferous parenchyma strands accompanied by fibers were a conspicuous bark feature observed in other barks (Carlquist 2002; Junikka and Koek-Noorman 2007; Şen et al. 2011; Quilhó et al. 2013; Mota et al. 2021; Sousa et al. 2021).

The rays, when observed in a transverse section, followed a straight to an undulated direction in the initial phloem but soon distorted due to the collapse of the sieve tubes and early formation of nodules of clusters sclereids (Fig. 3c); rays are non-storied, mainly uniseriate (Fig. 3a) and homogeneous with procumbent cells (Fig. 3d); the cells composing the phloem rays had thickened walls and dark contents (Fig. 3a). Dilatation of rays is moderate toward the bark outside (Fig. 3c).

The sclerenchyma tissue was abundant and formed a high proportion of *P. curatellifolia* bark; sclerenchyma is primarily in the form of sclereids and fiber-sclereids, and comparatively few fibers developed. A structural pattern in the nonconducting tissue of this species is recognized, starting with the formation of round and conspicuous nodules of cluster sclereids arranged more or less parallel to the vascular cambium that progressively becomes radially aligned and diminish towards the periphery (Figs. 1b and 3c). According to Roth (1981) the abundance of mechanical

tissue, especially in the form of sclereids, adds the hard and brittle consistency to the barks and constitutes a mechanical barrier against the collapse of living cells; this provides mechanical support of the tissue in the phloem of both tropical (Machado et al. 2005; Baptista et al. 2013) and temperate species (Şen et al. 2011; Cardoso et al. 2015; Vangeel et al. 2021).

Phenolic compounds were observed in rhytidome and nonconducting phloem by dark color staining in axial and ray parenchyma cells, cortical-like parenchyma, and sclereids (Fig. 1c and f). Crystals, presumably of calcium oxalate, mainly were present as prismatic crystals and found in parenchyma cells and sclereids (Figs. 3b and 4c). Starch grains were observed in our samples (Fig. 5a-b), as Halilu et al. (2008) also found in the bark of *Parinari* sp. Silica was also noticed (Fig. 3d), agreeing with records in the Flora Malesiana (1989) concerning the occurrence of silica in the phloem of *Chrysobalanaceae*. According to An and Xie (2022), few studies regarding phytoliths in bark exist. Still, the authors referred to studies in taxa from West Africa (Collura and Neumann 2017), where more than 90% of bark samples produced phytoliths, suggesting that silica production is concentrated in bark more than in wood.

Phenolic compounds and calcium oxalate crystals are common in the barks (Evert 2006) and, in conjunction with sclerenchyma, have evolved secondary defense functions (Franceschi et al. 2005).

3.3 Wood anatomical characterization

The general wood structure of *P. curatellifolia* resembles the structure of other *Parinari* species described in InsideWood (2004), i.e., *P. anamensis*, *P. campertis*, *P. congensis*, *P. excelsa*, concerning the type of wood porosity, vessel pits, axial parenchyma, the composition of the rays and presence of silica grains.

Growth rings are poorly distinct and marked by the thick-walled latewood fibers (Fig. 6b). The xylem produced by the vascular cambium is non-storied. It includes the vascular elements (conducting cells), the axial parenchyma (storage tissue), rays (storage/transversal conduction), and the fibers (mechanical support) (Figs. 6b, 7a and 8a).

Vessels were diffuse-porous, of two classes of diameter (Fig. 6b-d), exclusively solitary (> 90%), and tended to be oval in outline with the oblique arrangement. The mean tangential diameter was 155 µm (± 16), ranging between 56 and 277 µm, which is within the range of the values reported in the literature, i.e., 100–200 µm or ≥ 200 µm for *P. campestris* (InsideWood 2004). Simple perforation plates in horizontal end walls were observed (Fig. 6c-d). Vessel-ray pits are oblique and vertical (Fig. 6c), and inter-vessel pits are minute and alternate (Fig. 6c). Helical thickenings are absent. The mean vessel element length was 678 µm (± 44), with values between 342 and 915 µm, following the range reported for *Parinari* species: 350–800 µm (InsideWood 2004). Numerous vasicentric tracheids with distinctly bordered pits were observed, most conspicuous in tangential sections (Fig. 7b).

Axial parenchyma is non-storied in narrow bands up to 3 cells wide (Fig. 6b) and in strands of over 5 cells (Fig. 7a-b). The parenchyma cells were rectangular and pitted (Fig. 7c); spiral thickenings were not observed in our samples, agreeing with observations of Ter Welle (1975); this author mentioned the presence of spiral thickenings in most representative genera of the *Chrysobalanaceae*, but highlight the lack of spiral in the genus *Parinari*. Crystals were also absent.

Libriform fibers were generally non-septate (Figs. 6d and 7c) and aligned in a radial row when observed in the transverse section. Fibers were very pitted with bordered pits in radial and tangential walls (Figs. 7b and 8b) and well defined in individualized fibers (Fig. 8c). Bordered pits are signaled by Feitosa et al. (2012) in fibers of this species.

The mean fiber length was 1 363 µm (± 19), ranging between 934 and 1 673 µm, which is in the range of values reported for various genus of *Parinari*: 900–1600 µm

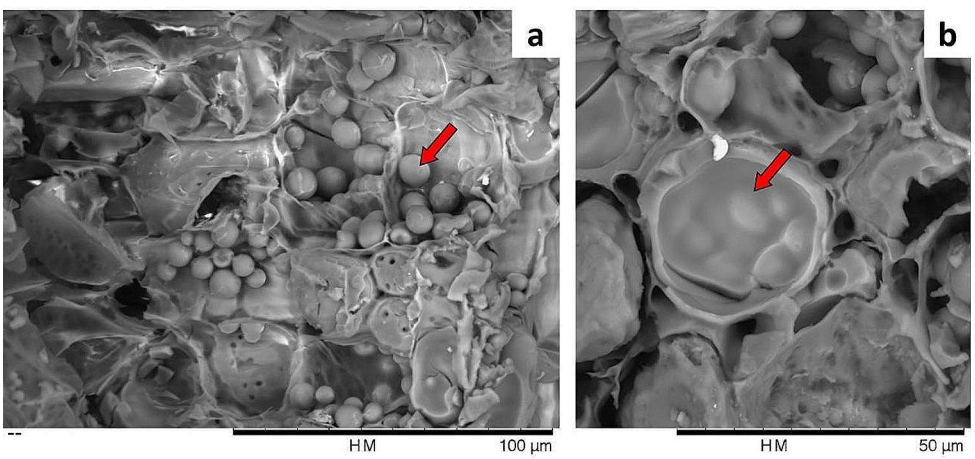


Fig. 5 Bark of *Parinari curatellifolia* under scanning electronic microscopy (SEM). Starch grain in parenchyma cells (arrow)

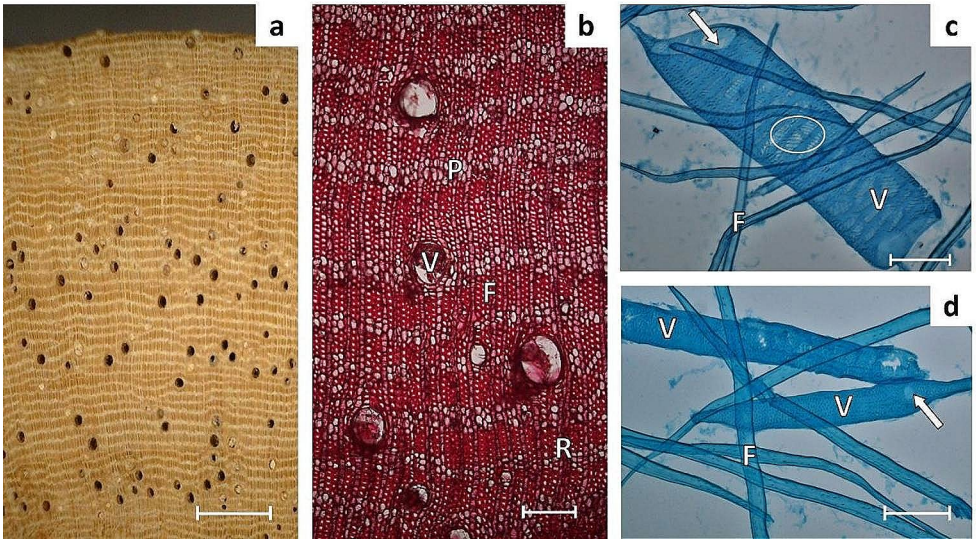


Fig. 6 Xylem of *Parinari curatellifolia*: **a**) Xylem observed under digital microscope Dino-Lite **b**) Vessel (V), axial parenchyma (P), fibers (F), ray (R); **c**) Large vessel element (V), sieve plate (arrow), vessel–ray pits (in a circle), fibers (F); **d**) Vessel (V), sieve plate (arrow), fibers (F). **a**, **b** (transverse section) **c**, **d** (maceration). Scale bar: **a** = 2 mm, **b** = 200 µm, **c**, **d** = 100 µm

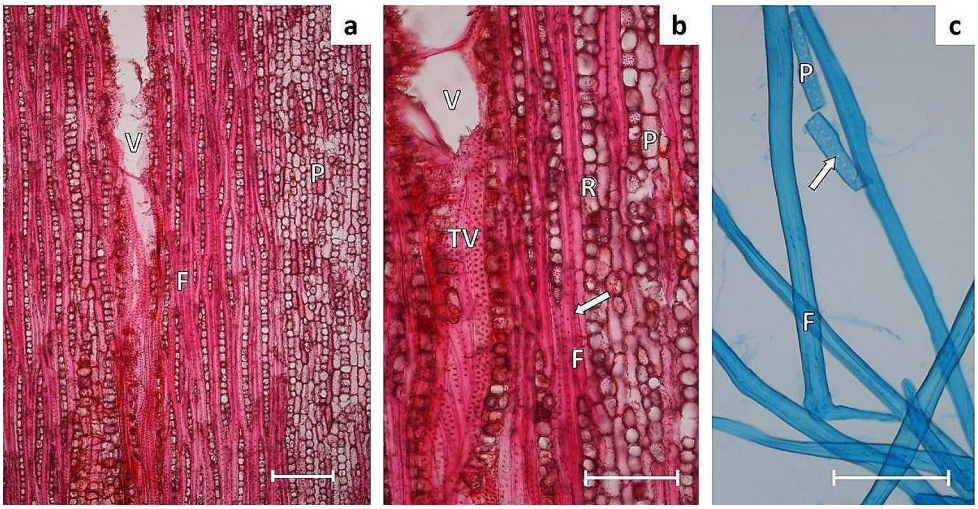


Fig. 7 Xylem of *Parinari curatellifolia* (tangential section): **a-b**) Vessel (V), axial parenchyma (P), fibers (F), ray (R), vascular tracheids (TV, in **b**); **c**) Axial parenchyma cells (P) with pits (arrow). **a**, **b** (tangential sections), **c** (maceration). Scale bar: **a** = 200 µm, **b**, **c** = 150 µm

(InsideWood 2004) although shorter than those referred to by Massuque et al. (2021b): 1.80 mm. The fibers mean width was 29 µm (±0.51), ranging from 18 to 42 µm; the fibers were thick-walled with a mean fiber wall thickness of 7 µm (±0.15), ranging between 4 and 10 µm. These fiber width and wall thickness values follow the literature for this species, i.e., 25.16 µm and 7.5 µm, respectively (Massuque et al. 2021b).

Rays were non-storied exclusively uniseriate (Fig. 7a-b) with a mean ray height of 440 µm (±22), ranging between 124 and 827 µm and 4–38 number of cells high. The rays were heterogeneous, with body ray cells procumbent with mostly 2–4 rows of upright and square marginal cells and sometimes rays with procumbent, square, and upright cells mixed throughout the ray (Fig. 8a-b). Radial canals were absent. Dark deposits were common in ray cells, but crystals were absent. Abundant silica was observed in ray cells and aggregations as irregularly shaped or globular bodies (Fig. 8b-c). Plants differ in their abilities to accumulate silica, varying significantly between species (Currie and Perry 2007). Silica bodies in ray cells were mentioned in various species of *Chrysobalanaceae*, i.e., *Licania leptostachya*, and as a diagnostic feature of species of different families, *i.e., Lauraceae*, *Dipterocarpaceae* (IAWA 1989). The role of phytoliths and microscopic amorphous silica structures as mechanical barriers against biotic and abiotic stress, and their use as taxonomic tools is highlighted by Nawaz et al. (2019).

Traumatic structures, i.e., pith fleck (Fig. 9a), presence of traumatic tyloses (Fig. 9b), and numerous traumatic thin vessels with tangential alignment (Fig. 9c), were detected, probably due in response to biotic or abiotic stress effects, i.e., drought, fire, insects, injury to the cambium that induces a disorganized formation of parenchymatous cells (IAWA 1964; Schweingruber 2007). According to Ceccantini (1996) and Mota et al. (2017), water deficits may cause the formation of pith flecks.

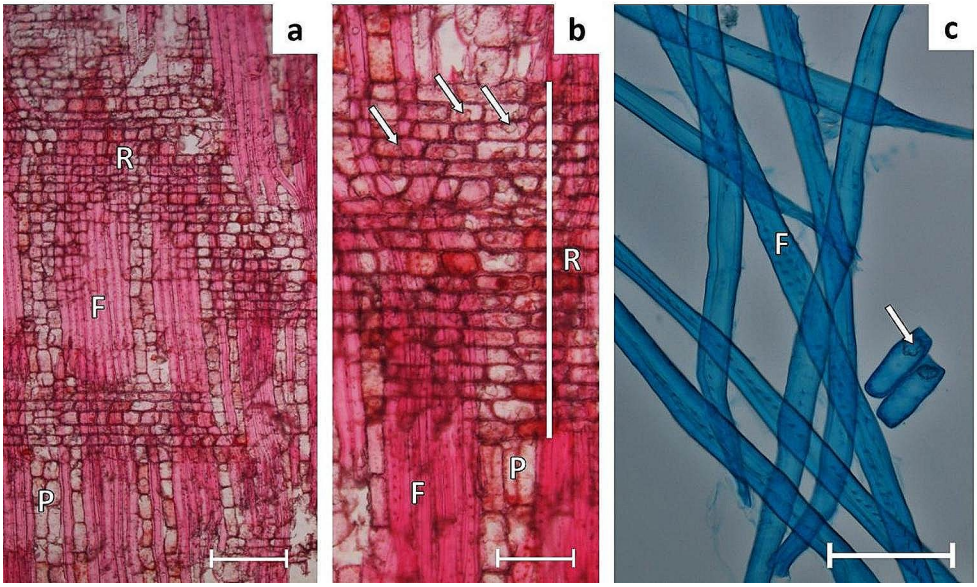


Fig. 8 Xylem of *Parinari curatellifolia*: **a-b**) Axial parenchyma (P), fibers (F), rays (R); silica grains (arrows, in **b**), **c**) Radial parenchyma cells with silica grains (arrow), fibers (F). **a**, **b** (Radial sections), **c** (maceration). Scale bar: **a** = 200 µm, **b** = 150 µm, **c** = 100 µm

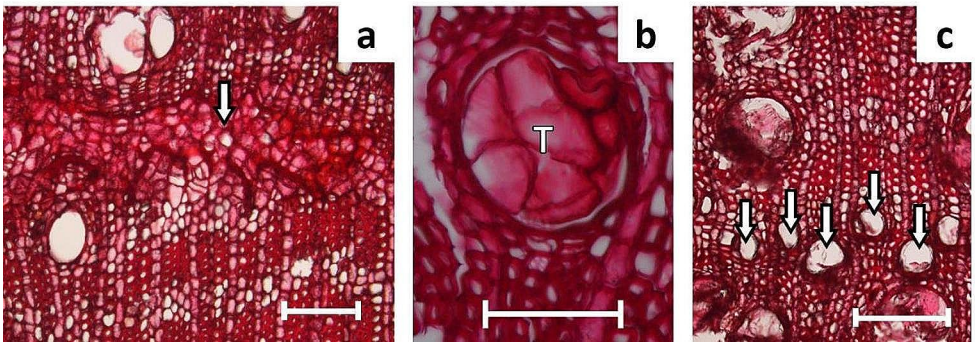


Fig. 9 Traumatic structure in the xylem of *Parinari curatellifolia*: **a**) Pith fleck (arrow) observed in transverse section (arrow); **b**) Tyloses (T); **c**) Thin vessels with tangential alignment (arrows). Scale bar: **a** = 200 µm, **b** = 100 µm, **c** = 200 µm

3.4 Cell size variation of the secondary phloem and xylem between trees

Wood and bark are heterogeneous materials due to their biological origin (Zobel and van Buijtenen 1989). Their formation involves production and growth of new cells by the vascular cambium and their subsequent differentiation, induced by hormonal signals, i.e., auxin, cytokinin, and gibberellin (Aloni 2021) and affected not only by internal aspects but also by external factors i.e. site and ecological (Zobel and van Buijtenen 1989; Meinzer et al. 2011; Benhura et al. 2013; Gricar et al. 2015). In addition, the dimensions of xylem and phloem cells have been shown to vary as a function of tree age, height, or tree diameter (Quilhó et al. 2000; Petit and Crivellaro 2014; Clerx et al. 2020), giving rise to variations in cell structure between trees in most species.

Table 1 summarizes the cell dimensions in the bark and wood of *P. curatellifolia* in studied trees. For bark, the height of the rays, the length and tangential diameter of the sieve-tube elements, and the length and lumen of the fibers were significantly different ($p < 0.05$) between trees; also, for wood ANOVA revealed significant differences ($p < 0.05$) concerning rays (height and nº cells), vessel elements (length and tangential diameter), and fiber (length, width, and lumen) among trees.

According to the results and when comparing the cell dimensions between bark and wood, the wood has larger cells than the bark (Table 1); i.e., bark fibers are shorter than those of the wood (on average, 1363.30 µm in wood and 1245.47 in bark) agreeing with Quilhó et al. (2013) in *Quercus faginea*, but in opposition to the results found in tropical trees by Parameswaran and Liese (1974) and in *Eucalyptus globulus* by Jorge et al. (2000).

There are few records concerning the correlation between xylem and phloem cells. Most were correlated with changes in conduit diameter, i.e., sieve tube diameter was strongly correlated with vessel diameter (Jacobsen et al. 2018). Still, our results also show that trees with large vessels have narrow sieve tube elements. Unfortunately, studies concerning bark and wood cell size variations between trees in *Parinari* sp. were not found in the literature.

Table 1 Biometric data for bark and wood of *P. curatellifolia* after individualization (mean values of three threes)

Bark		1	2	3
Sieve tube elements	Length (µm)	(375.90) [c]	(385.82) [b]	(507.71) [a]
	Tangential diameter (µm)	(31.83) [a]	(22.03) [b]	(20.65) [b]
Fibers	Length (µm)	(1319.93) [a]	(1220,74) [b]	(1195.73) [c]
	Width (µm)	(26.29) [a]	(25.45) [a]	(25.66) [a]
	Lumen (µm)	(12.37) [b]	(12.75) [c]	(12.92) [a]
	Wall thickness (µm)	(6.96) [a]	(6.35) [a]	(6.37) [a]
Rays	Height (in n◦ cells)	(11.36) [a]	(10.40) [a]	(11.00) [a]
	Height (µm)	(393.76) [c]	(399.19) [b]	(434.55) [a]
Wood		1	2	3
Vessel elements	Length (µm)	(562.45) [c]	(728.96) [b]	(741,32) [a]
	Tangential diameter (µm)	(134.93) [c]	(158.18) [b]	(170.53) [a]
Fibers	Length (µm)	(1261.56) [a]	(1434.28) [b]	(1394.04) [c]
	Width (µm)	(27.76) [b]	(26.59) [b]	(32.30) [a]
	Lumen (µm)	(15.61) [b]	(12.34) [c]	(17.56) [a]
	Wall thickness (µm)	(6.08) [a]	(6.12) [a]	(6.36) [a]
Rays	Height (in n◦ cells)	(17.20) [a]	(13.72) [b]	(16.32) [a]
	Height (µm)	(413.37) [c]	(434.43) [b]	(473.15) [a]

Average values followed by the same letter are not significantly different ($p < 0.05$)

Table 2 Chemical summative analysis (in percentage oven-dry mass) of wood and bark from *P. curatellifolia*

Components (% of o.d. mass)	Wood	Bark
Ash	1.6 ± 0.1	3.2 ± 0.3
Total extractives	10.0 ± 0.1	12.2 ± 0.2
Dichloromethane	0.3	0.9
Ethanol	6.9	8.6
Water	2.7	2.7
Suberin	-	5.4 ± 0.3
Total lignin	28.4 ± 0.7	42.4 ± 1.6
Klason lignin	27.5	4.4
Soluble lignin	0.9	1.0
Total Sugars	52.8 ± 4.9	42.5 ± 8.1
Rhamnose	0.2	0.1
Arabinose	0.4	0.8
Galactose	1.0	0.9
Glucose	36.5	26.7
Xylose	11.0	10.6
Mannose	-	-
Galacturonic acid	1.5	1.4
Glucuronic acid	-	-
Acetic acid	2.2	1.2

Mean of three-replicate ± standard deviation of the wood and bark samples

3.5 Basic density

As expected, the basic density of wood was higher than bark (580 vs. 505 kg m^{-3}). *P. curatellifolia*, wood density values reported reached 593 $kg.m^{-3}$ (Abbot et al. 1997) and 720 $kg.m^{-3}$ (Orwa et al. 2009), which is in accordance with our results. However, no studies on the density of the bark were found. Density is crucial in determining a feedstock's economics and fuel quality since it affects transport costs, combustion performance, and energy per volume.

3.6 Chemical composition

Chemical summative analysis of wood and bark from *P. curatellifolia* is presented in Table 2.

The bark contains suberin in 5.4% (but no data about its chemical composition is available), a higher content in ash (3.2%), lignin (42.4%), and extractives (12.2%, where polar compounds make up 70.5% of the total); and a moderate content in polysaccharides (42.5%). Conversely, wood has a lower extractives content (10%), ash (1.6%), lignin (28.4%), and polysaccharides (52.8%), compared to bark and the values reported in the literature: 3.21% extractives, 2.55% ash, 29.59% lignin and 64.64% polysaccharides (Massuque et al. 2020). The differences could be attributed to geographical location, soil, and climate conditions, as Benhura et al. (2013) suggested. In general, *P. curatellifolia* presented a higher lignin content when compared with other miombo species, such as *Julbernardia globiflora* (23.8%), *Brachystegia spiciformis* (24.8%), *Brachystegia boehmii* (25.9%) and very similar to the species *Uapaca kirkiana* (29.4%), *Pericopsis angolensis* (29,2%) (Sangumbe et al. 2018; Massuque et al. 2021a).

3.7 Lipophilic extracts composition

The quantitative proportions of the chemical families identified by GC-MS in the DCM extracts of wood and bark are presented in Table 3. It was possible to identify about 92.2% (from wood) and 90.3% (from bark) of the total ion

Table 3 The proportion of chemical families in the lipophilic dichloromethane extracts (as a percentage of total area) identified by GC–MS in wood and bark from *P. curatellifolia*

	Wood	Bark
n-Alkanols	0.27	0.60
Fatty acids (saturated, unsaturated)	86.16	8.25
ω-Hidroxyacids	2.46	0.61
Aromatics	0.26	0.96
Phytosterols	1.29	8.78
Triterpenoids	0.41	67.67
Sugars	0.04	0.03
Glycerol + derivatives	1.16	0.22

chromatogram area; there is a distinct difference in chemical composition between wood and bark. The wood revealed a high content of fatty acids (86.2%), where de hexadecanoic acid ($C_{16:0}$), 9,12-octadecadienoic acid ($C_{18:2}$), 9-octadecenoic acid ($C_{18:1}$) and octadecanoic acid ($C_{18:0}$) respectively with 28.4%, 17.2%, 30.8%, and 5.1% were the predominant compounds. In turn, the bark is rich in triterpenoids compounds (67.7%), where betulinic acid (32.2%), corosolic acid (10.1%), ursolic acid (8.8%), and oleanolic acid (6.5%) were identified as the main compounds. It is not easy to compare the results obtained since, to our knowledge, this is the first study reporting the lipophilic profile of *P. curatellifolia*. Various studies focus on the phytochemical screening of plant fractions from *P. curatellifolia*, such as leaves, barks, wood, seeds, and roots with different polar solvents. These studies have identified the presence of saponins, alkaloids, flavonoids, steroids, and tannins (Ogunbolude et al. 2009; Peni et al. 2010).

3.8 Phytochemical profile and antioxidant activity of ethanol/water extracts

The yield of the extraction ethanol:water (80:20, v/v), phytochemical profile, and antioxidant activity are presented in Table 4. The extraction yield was similar between wood (8.57%) and bark (8.29%) and slightly lower than the content of the polar extractives determined by sequential solvent extraction (9.6% for wood and 11.3% for bark, Table 2). The Soxhlet apparatus can attribute this result. The sample is repeatedly brought into contact with fresh portions of solvent, and the system remains at a relatively high temperature, furthermore, no filtration is required after leaching, and sample yield can be increased by performing several simultaneous extractions (Luque de Castro and Priego-Capote 2010).

Bark presented the higher values for the phytochemical profile: total phenolics (443.8 mg GAE/g extract), flavonoids (461.0 mg CE/g extract), and condensed tannins (287.7 mg CE/g extract) in comparison with wood (102 mg GAE/g extract, 72.8 and 55.5 mg CE/g extract, Table 4).

Table 4 Phytochemical profile values (total phenolics, total flavonoids, condensed tannins) and wood and bark's antioxidant properties (FRAP and DPPH) from *P. curatellifolia*

	Wood	Bark
Extraction yield (%)	8.6 ± 0.9	8,3 ± 0.7
Phytochemical profile		
Total phenolics (mg GAE/g extract)	102.0 ± 13.3	443.8 ± 86.3
Total flavonoids (mg CE/g extract)	72.8 ± 14.5	461.0 ± 90.2
Condensed tannins (mg CE/g extract)	55.5 ± 14.5	287.7 ± 49.2
Antioxidant activity		
DPPH Antioxidant capacity (mg TEAC/g extract)	459.6 ± 98.7	1410.0 ± 285.1
DPPH IC50 values (µg extract/ml)	8.5 ± 1.6	2.8 ± 0.5
DPPH AAI	2.9 ± 0.6	8.8 ± 1.8
FRAP (mM TEAC/g extract)	0.9 ± 0.1	4.7 ± 0.6

Mean of three-replicate ± standard deviation of the wood and bark samples. IC50: Trolox in ethanol-water 3.76 µg Trolox/ml; TEAC: Trolox equivalents antioxidant; GAE: gallic acid equivalents; CE: catechin equivalents

Generally, bark presents high contents of total phenolics (Ferreira et al. 2018).

Regarding the antioxidant activities, bark also presented higher FRAP values than wood (4.7 vs. 0.9 mM TEAC/g extract) and the same DPPH (1410 vs. 459 mg TEAC/g extract, Table 4). The antioxidant capacity expressed by AAI value was 8.8 in bark and 2.8 for wood, corresponding to a very strong antioxidant classification since AAI > 2 (Neiva et al. 2018). Overall, both tissues are interesting to be used as feedstock for antioxidant extraction and bio-based product development.

3.9 Analytical pyrolysis

The results from analytical pyrolysis are presented in Table 5, where generally, there were no great differences between trees, so only the mean values will be presented and discussed. Bark presented higher content in lignin-derived compounds (33.0 vs. 31.8%) but lower carbohydrate derivatives when compared to wood (42.5 vs. 47.7%). In both tissues, the main compound identified was levoglucosan (peak 72, presented in Table SI 1), representing 7.6 (bark) and 8.8% (wood) of the total pyrogram area. Levoglucosan results from the depolymerization process of dehydrated cellulose (Dobele et al. 1999), and its yield is influenced by the cellulose characteristics, pyrolysis conditions, and inorganic compounds (Lourenço et al. 2019). The lignin in both bark and wood was mainly composed of guaiacyl and syringyl-units, reflected in the S/G ratio, whose values were 0.2 and 0.4, typical of hardwoods (Lourenço et al. 2019) and comparable to the values 0.35 attained by alkaline oxidation

Table 5 Quantification of the pyrolysis-derived compounds from wood and bark of *P. curatellifolia* (% of total pyrogram area). Mean of three-replicate ± standard deviation of the wood and bark samples

	Wood	Bark
Total carbohydrates	47.7 ± 3.05	42.5 ± 0.51
Total lignin	31.8 ± 1.45	33.0 ± 1.09
H	0.7 ± 0.14	1.3 ± 0.52
G	22.5 ± 3.12	25.9 ± 0.62
S	8.5 ± 1.58	5.7 ± 0.61
Other LDC	1.5 ± 0.16	3.2 ± 0.30
others	0.4 ± 0.16	0.3 ± 0.12
C/L ratio	1.4 ± 0.13	1.2 ± 0.03
S/G ratio	0.4 ± 0.15	0.2 ± 0.02
H:G:S relation	1:35:12	1:22:5

Other LDC – other compounds assigned to lignin but not with H, G, S-lignin units (e.g., catechol, orcinol)

Table 6 Proximate analysis and ultimate analysis present in wood and bark from *P. curatellifolia*. Mean values of three-replicate

			Mineral composition (mg/kg)		
Proximate analysis	*Wood*	*Bark*		*Wood*	*Bark*
Moisture content (%)	8.0	9.0	Na	32.2	30.7
Ash (%)	1.6	3.3	K	2387.8	2560.3
Total Volatiles (%)	20.7	27.5	Ca	912.3	6509.2
Fixed carbon (%)	77.7	69.1	Mg	874.6	374.9
HHV (MJ/kg)	19.1	20.9	P	237.7	97.5
			S	152.5	209.1
Ultimate analysis	*Wood*	*Bark*	Fe	24.2	51.5
C (%)	45.7	48.7	Cu	2.2	4.7
H (%)	6.1	5.8	Zn	2.1	2.01
N (%)	0.1	0.3	Mn	4.0	5.5
O (%)	48.1	45.2	B	2.9	7.5
H/C ratio	0.13	0.12	Cr	2.3	3.7
O/C ratio	1.05	0.93	Ni	2.0	1.2
			Cd	0.02	-
			Pb	2.6	2.3

of *Parinari curatellifolia* wood (Massuque et al. 2021a), but lower compared to 0.89 and 1.72 attained by oxidation with copper (II) oxide of *Brachystegia spiciformis* and *Pericopsis angolensis* other Miombo species (Sangumbe et al. 2018). In bark, the H:G:S monomeric composition was 1:22:5, while in wood, it was 1:35:12, revealing a slightly higher content of guaiacyl units in bark (25.9 vs. 22.5%) and more syringyl units in wood (8.5 vs. 5.7%). Still, both had minor amounts of H-units (0.7 vs. 1.3 in wood and bark, respectively). The results of pyrolysis and wet chemistry analysis are different regarding lignin content. The difference was 5.2% for wood samples, similar to the ones reported by Costa et al. (2023). According to the previous author, this difference (6.1%) is mainly due to the formation of low molecular compounds during pyrolysis that can be produced either from carbohydrates or lignin but mainly accounts for the carbohydrate's sum.

3.10 Proximate analysis and ultimate analysis

Table 6 presents the proximate, ultimate analysis, higher heating value (HHV), and mineral composition of *P. curatellifolia* samples. Generally, the bark had higher moisture content (9.0 vs. 8.0%), ash (3.3 vs. 1.6%), total volatiles (27.5 vs. 20.7%), and less fixed carbon (69.1 vs. 77.7%) compared to wood. The wood values are similar to the literature, except for ash content of 6.8%, the total volatiles of 21.5%, and fixed carbon of 71.7% (Massuque et al. 2021a). The higher ash content in the bark is a problem for biofuel production since they are responsible for the sintered molten deposit in the biomass boilers (Labbé et al. 2020).

The ultimate analysis presented more similar values between bark and wood, e.g., the ratio between hydrogen and carbon in bark and wood (0.12 vs. 0.13) and the ratio between oxygen and carbon (0.93 vs. 1.05). Bark presented slightly higher carbon content (48.7%) than wood (45.7%), but wood presented more oxygen than bark (48.1 vs. 45.2%). Interestingly, the hydrogen content was similar in both tissues (5.8 vs. 6.1%), while bark presented more than double nitrogen content (0.3%). Some of the data obtained here is similar to the literature: both bark and wood presented similar hydrogen 5.58%, but differ slightly in carbon (48.7 vs. 47.4%), nitrogen (0.3 vs. 0.9%), and oxygen (45.2 vs. 45.8%) (Massuque et al. 2020).

Regarding the HHV, there is not much difference between bark and wood (20.9 vs. 19.1 MJ/kg), but for wood of *P. curatellifolia*, there was reported a lower value of 18.5 MJ/kg (Massuque et al. 2020), slightly lower than 20.0 MJ/kg from wood of *B. spiciformis* and *B. utilis*, the favorite species of rural communities (Menéndez and Curt 2013). For the mineral composition, the most important minerals were potassium (2560.3 and 2387.8 mg/kg), calcium (6509.2 and 912.3 mg/kg), and magnesium (374.9 and 874.6 mg/kg), respectively, in bark and wood. The mineral composition is similar in fruits and seeds (Benhura et al. 2013; Lesten et al. 2018).

4 Conclusion

Parinari curatellifolia is well known within rural communities in Huambo-Angola for providing firewood, charcoal, and fruit. As far as we know, this is the first time this species has been characterized in terms of anatomy and chemistry, particularly for bark tissue. In contrast, few studies have been conducted on wood chemistry, and none have been conducted on its anatomy. Chemically, bark has considerable suberin, extractives, lignin contents, and high antioxidant activity compared to wood. Therefore, local communities should use bark extraction for traditional medicine and industrial purposes to

increase the potential valorization of P. *curatellifolia* under the biorefineries framework. The wood's chemical composition, particularly lignin content and composition (more G-units), and its proximate values (e.g., high HHV) confirmed its good properties for energy, which is now the traditional use. Still, its characteristics favored the production of more value-added products under the scope of bio-energy, such as biocarbon (also known as charcoal and produced more efficiently), and also bio-chemicals with phytochemistry and pharmacology activities that could be attained from sustainable and managed forests to preserve this species. Therefore, *P. curatellifolia* biomass could be integrated into a biorefinery context to provide socio-economic benefits to rural communities seeking to fulfill the Sustainable Development Goals of the United Nations.

Supplementary Information The online version contains supplementary material available at https://doi.org/10.1007/s00107-024-02074-2.

Acknowledgements This research was funded by Instituto Nacional de Gestão de Bolsas de Estudos da República de Angola (INAGBE) by Bolsas de Mérito Edição-2019. Was also supported by FCT (Fundação para a Ciência e Tecnologia, Portugal) by financing the Forest Research Center (UIDB/00239/2020 and UIDP/00239/2021), Ana Lourenço through a research contract (DL 57/2016/CP1382/CT0007), Ricardo Costa acknowledges a doctoral fellowship with reference 2020.07451.BD. The first author would also like to recognize the staff of FCA and UJES in Huambo province. The authors also acknowledge António V. Marques for his personal database of the TMS compounds mass spectra for GC.

Author contributions J.G., T.Q., and A.M. designed the work. A.M. wrote the main manuscript text. A.L., H.P., R.A.C., T.Q., J.G. edited the main manuscript text. T.Q., H.P., and A.M. realized the anatomical features and interpreted the results. A.M., R.A.C., A.L., and J.G. performed the chemical analyses and interpretation of data. All authors agreed on the final version to be published.

Funding Open access funding provided by FCT|FCCN (b-on).

Declarations

Competing interests The authors declare that they have no known competing financial interests or personal relationships that could have appeared to influence the work reported in this paper.

Open Access This article is licensed under a Creative Commons Attribution 4.0 International License, which permits use, sharing, adaptation, distribution and reproduction in any medium or format, as long as you give appropriate credit to the original author(s) and the source, provide a link to the Creative Commons licence, and indicate if changes were made. The images or other third party material in this article are included in the article's Creative Commons licence, unless indicated otherwise in a credit line to the material. If material is not included in the article's Creative Commons licence and your intended use is not permitted by statutory regulation or exceeds the permitted use, you will need to obtain permission directly from the copyright holder. To view a copy of this licence, visit http://creativecommons.org/licenses/by/4.0/.

References

Abbot P, Lowore J, Khofi C, Werren M (1997) Defining firewood quality: a comparison of quantitative and rapid appraisal techniques to evaluate firewood species from a southern African Savanna. Biomass Bioenergy 12:429–437. https://doi.org/10.1016/S0961-9534(96)00084-0

Aloni R (2021) Hormonal Control of Reaction Wood Formation. Vascular differentiation and plant hormones. Springer International Publishing, Cham, pp 265–272

An X, Xie B (2022) Phytoliths from Woody plants: a review. Divers (Basel) 14:339. https://doi.org/10.3390/d14050339

Angyalossy V, Pace MR, Evert RF et al (2016) IAWA List of Microscopic Bark features. IAWA J 37:517–615. https://doi.org/10.1163/22941932-20160151

ASTM (2013) ASTM D5373-08. Standard test methods for Instrumental determination of Carbon, Hydrogen, and Nitrogen in Laboratory samples of coal. ASTM International, West Conshohocken

ASTM (2019) ASTM E870-82. Standard test methods for analysis of Wood fuels. ASTM International, West Conshohocken

Baptista I, Miranda I, Quilhó T et al (2013) Characterisation and fractioning of *Tectona grandis* bark in view of its valorisation as a biorefinery raw-material. Ind Crops Prod 50:166–175. https://doi.org/10.1016/j.indcrop.2013.07.004

Barbosa ACF, Pace MR, Witovisk L, Angyalossy V (2010) A new method to obtain good anatomical slides of heterogeneous plant parts. IAWA J 31:373–383. https://doi.org/10.1163/22941932-90000030

Benhura M, Muchuweti M, Gombiro P, Benhura C (2013) Properties of (*Parinari Curatellifolia*) (Hacha or Chakata) fruits from different parts of Harare, Zimbabwe. Afr J Food Agric Nutr Dev 13:8004–8018. https://doi.org/10.18697/ajfand.59.12520

Bolza E, Keating WG (1972) African timbers: the properties, uses and characteristics of 700 species. Commonwealth scientific and industrial research organization, Melbourne

Cardoso S, Sousa VB, Quilhó T, Pereira H (2015) Anatomical variation of teakwood from unmanaged mature plantations in East Timor. J Wood Sci 61:326–333. https://doi.org/10.1007/s10086-015-1474-y

Carlquist S (2002) Wood and Bark anatomy of Salvadoraceae: Ecology, relationships, Histology of Interxylary Phloem. J Torrey Bot Soc 129:10. https://doi.org/10.2307/3088678

Carnevale Neto F, Pilon AC, Da Silva Bolzani V, Castro-Gamboa I (2013) Chrysobalanaceae: secondary metabolites, ethnopharmacology and pharmacological potential. Phytochem Rev 12:121–146. https://doi.org/10.1007/s11101-012-9259-z

Ceccantini G (1996) Anatomia ecológica do lenho de espécies de cerrado e mata: *Casearia sylvestris* Sw. e *Machaerium villosum* Vog. (Ecological anatomy of wood from cerrado and forest species: *Casearia sylvestris* Sw. and *Machaerium villosum* Vog). Dissertação Mestrado, Universidade de São Paulo

Chiteculo V, Abdollahnejad A, Panagiotidis D, Surový P (2022) Effects, Monitoring and Management of Forest roads using remote sensing and GIS in Angolan Miombo Woodlands. Forests 13. https://doi.org/10.3390/f13040524

Clerx LE, Rockwell FE, Savage JA, Holbrook NM (2020) Ontogenetic scaling of phloem sieve tube anatomy and hydraulic resistance with tree height in *Quercus rubra*. Am J Bot 107:852–863. https://doi.org/10.1002/ajb2.1481

Collura LV, Neumann K (2017) Wood and bark phytoliths of west African woody plants. Quatern Int 434:142–159. https://doi.org/10.1016/j.quaint.2015.12.070

Costa RA, Lourenço A, Patrício H et al (2023) Valorization of Pine Nut Industry residues on a Biorefinery Concept. https://doi.org/10.1007/s12649-023-02068-w. Waste Biomass Valorization

Currie HA, Perry CC (2007) Silica in plants: Biological, biochemical and chemical studies. Ann Bot 100:1383–1389. https://doi.org/10.1093/aob/mcm247

Delgado-Matas C, Pukkala T (2015) Growth models for six *Eucalyptus* species in Angola. South for 77:141–152. https://doi.org/10.2989/20702620.2014.984266

Dobele G, Rossinskaja G, Telysheva G et al (1999) Cellulose dehydration and depolymerization reactions during pyrolysis in the presence of phosphoric acid. J Anal Appl Pyrol 49:307–317. https://doi.org/10.1016/S0165-2370(98)00126-0

Evert RF (2006) Esau's plant anatomy, 3rd edn. John Wiley & Sons, Inc., Hoboken, NJ, USA

Faix O, Meier D, Fortmann I (1990) Thermal degradation products of wood–gas chromatographic separation and mass spectrometric characterization of monomeric lignin derived products. Holz Roh- Werkst 48:281–285. https://doi.org/10.1007/BF02626519

Feitosa EA, Xavier HS, Randau KP (2012) Chrysobalanaceae: traditional uses, phytochemistry and pharmacology. Revista Brasileira De Farmacognosia 22:1181–1186. https://doi.org/10.1590/S0102-695X2012005000080

Ferreira JPA, Miranda I, Sousa VB, Pereira H (2018) Chemical composition of barks from *Quercus faginea* trees and characterization of their lipophilic and polar extracts. PLoS ONE 13:1–18. https://doi.org/10.1371/journal.pone.0197135

Flora Malesiana (1989) Chrysobalanaceae | Flora Malesiana. https://portal.cybertaxonomy.org/flora-malesiana/cdm_dataportal/taxon/a8b430fe-f50f-4871-bff0-c348ecfe05de. Accessed 17 Aug 2023

Franceschi VR, Krokene P, Christiansen E, Krekling T (2005) Anatomical and chemical defenses of conifer bark against bark beetles and other pests. New Phytol 167:353–376. https://doi.org/10.1111/j.1469-8137.2005.01436.x

Franklin GL (1945) Preparation of Thin sections of Synthetic resins and Wood-Resin composites, and a New Macerating Method for Wood. Nature 155:51–51. https://doi.org/10.1038/155051a0

Gaudino S, Galas C, Belli M et al (2007) The role of different soil sample digestion methods on trace elements analysis: a comparison of ICP-MS and INAA measurement results. Accred Qual Assur 12:84–93. https://doi.org/10.1007/s00769-006-0238-1

Gominho J, Costa RA, Lourenço A et al (2021) *Eucalyptus globulus* Stumps Bark: chemical and anatomical characterization under a Valorisation Perspective. Waste Biomass Valorization 12:1253–1265. https://doi.org/10.1007/s12649-020-01098-y

Gororo M, Chimponda T, Chirisa E, Mukanganyama S (2016) Multiple cellular effects of leaf extracts from *Parinari Curatellifolia*. BMC Complement Altern Med 16:1–14. https://doi.org/10.1186/s12906-016-1287-6

Gricar J, Prislan P, De Luis M et al (2015) Plasticity in variation of xylem and phloem cell characteristics of Norway spruce under different local conditions. Front Plant Sci 6:1–14. https://doi.org/10.3389/fpls.2015.00730

Halilu ME, Akpulu IK, Agunu A et al (2008) Phytochemical and antibacterial evaluation of *Parinari Curatellifolia* Planch Ex Benth (Chrysobalanaceae). Nigerian J Basic Appl Sci 16:281–285

Halilu ME, October N, Balogun M et al (2013) Isolation and characterization of steroids from petroleum ether extract of stem bark of *Parinari Curatellifolia* Planch ex. Benth (Chrysobalanaceae). J Nat Sci Res 3:53–61

IAWA (1964) Multilingual glossary of terms used in wood anatomy. Verlagsanstalt Buchdruckerei Konkordia, Winterthur

IAWA (1989) List of microscope features for hardwood identification. IAWA Bull 10:219–332

InsideWood (2004) The Inside Wood Database. http://insidewood.lib.ncsu.edu/search;jsessionid=6EFC258CE80E8ACB7CD03F274EF59FD4?0. Accessed 17 Aug 2023

Jacobsen AL, Valdovinos-Ayala J, Rodriguez-Zaccaro FD et al (2018) Intra-organismal variation in the structure of plant vascular transport tissues in poplar trees. Trees - Struct Function 32:1335–1346. https://doi.org/10.1007/s00468-018-1714-z

Jorge F, Quilhó T, Pereira H (2000) Variability of fibre length in wood and bark in *Eucalyptus globulus*. IAWA J 21:41–48. https://doi.org/10.1163/22941932-90000235

Junikka L (1994) Survey of English macroscopic bark terminology. IAWA J 15:3–45

Junikka L, Koek-Noorman J (2007) Anatomical structure of barks in neotropical genera of Annonaceae. Ann Bot Fenn 44:79–132

Kundishora A, Sithole S, Mukanganyama S (2020) Determination of the cytotoxic effect of different Leaf extracts from Parinari Curatellifolia (Chrysobalanaceae). J Toxicol 2020. https://doi.org/10.1155/2020/8831545

Labbé R, Paczkowski S, Knappe V et al (2020) Effect of feedstock particle size distribution and feedstock moisture content on pellet production efficiency, pellet quality, transport and combustion emissions. Fuel 263. https://doi.org/10.1016/j.fuel.2019.116662

Lesten ECC, Kingsley M, Macdonald J (2018) Proximate composition, physical characteristics and mineral content of fruit, pulp and seeds of *Parinari Curatellifolia* (Maula) from Central Malawi. Afr J Food Sci 12:238–245. https://doi.org/10.5897/ajfs2017.1662

Lhate I, Cuvilas C, Terziev N, Jirjis R (2010) Chemical composition of traditionally and lesser used wood species from Mozambique. Wood Mater Sci Eng 5:143–150. https://doi.org/10.1080/17480272.2010.484867

Lourenço A, Gominho J, Pereira H (2019) Chemical Characterization of Lignocellulosic Materials by Analytical Pyrolysis. In: Analytical Pyrolysis. IntechOpen

Luque de Castro MD, Priego-Capote F (2010) Soxhlet extraction: past and present panacea. J Chromatogr A 1217:2383–2389. https://doi.org/10.1016/j.chroma.2009.11.027

Machado SR, Marcati CR, De Morretes BL, Angyalossy V (2005) Comparative bark anatomy of root and stem in *Styrax Camporum* (Styracaceae). IAWA J 26:477–487. https://doi.org/10.1163/22941932-90000129

Maharaj V, Glen H (2008) *Parinari curatellifolia* | Plantz Africa. KZN Herbarium, South African National Biodiversity Institution Plant Information Website. q=Maharaj V%2 C Glen HF %282008%29 Parinari curatellifolia%2 C KZN Herbarium%2 C South African National Biodiversity Institution Plant Information Website. https://scholar.google.com/scholar?&

Malengue AS, Miranda I, Simões R et al (2023) Cork cellular and chemical features underlying bark environmental protection in the miombo species *Parinari curatellifolia*. Heliyon 9:e21135. https://doi.org/10.1016/j.heliyon.2023.e21135

Massuque J, De Assis MR, Trugilho PF (2020) Characterization of Miombo species used by rural communities as fuelwood in Northern Mozambique. Energy Sources Part A: Recovery Utilization Environ Eff 00:1–10. https://doi.org/10.1080/15567036.2020.1815910

Massuque J, De Assis MR, Loureiro BA et al (2021a) Influence of lignin on wood carbonization and charcoal properties of Miombo Woodland native species. Eur J Wood Product 79:527–535. https://doi.org/10.1007/s00107-021-01669-3

Massuque J, de Sousa KIR, Trugilho PF (2021b) Effect of fibre and vessel biometry on wood combustibility of native Miombo tree species. South Forests: J for Sci 83:269–275. https://doi.org/10.2989/20702620.2021.1994341

Mawire P, Mozirandi W, Heydenreich M et al (2021) Isolation and antimicrobial activities of phytochemicals from Parinari Curatellifolia (Chrysobalanaceae). Adv Pharmacol Pharm Sci 2021. https://doi.org/10.1155/2021/8842629

Meinzer FC, Lachenbruch B, Dawson TE (2011) Size- and Age-related changes in Tree structure and function. Springer, Dordrecht

Menéndez A, Curt MD (2013) Energy and socio-economic profile of a small rural community in the highlands of central Tanzania: a case study. Energy Sustain Dev 17:201–209. https://doi.org/10.1016/j.esd.2012.12.002

Metcalfe CR, Chalk L (1950) Anatomy of the dicotyledons: leaves, stem, and wood, in relation to taxonomy, with notes on economic uses. Clarendon, Oxford

Miapia LM, Ariza-Mateos D, Lacerda-Quartín V, Palacios-Rodríguez G (2021) Deforestation and Biomass Production in Miombo Forest in Huambo (Angola): a balance between local and global needs. Forests 12:1557. https://doi.org/10.3390/f12111557

Miranda I, Lima L, Quilhó T et al (2016) The bark of *Eucalyptus sideroxylon* as a source of phenolic extracts with anti-oxidant properties. Ind Crops Prod 82:81–87. https://doi.org/10.1016/j.indcrop.2015.12.003

Mota GS, Sartori CJ, Miranda I et al (2017) Bark anatomy, chemical composition and ethanol-water extract composition of *Anadenanthera peregrina* and *Anadenanthera colubrina*. PLoS ONE 12:1–14. https://doi.org/10.1371/journal.pone.0189263

Mota GS, Sartori CJ, Ribeiro AO et al (2021) Bark characterization of *Tachigali guianensis* and *Tachigali Glauca* from the Amazon under a valorization perspective. BioResources 16:2953–2970. https://doi.org/10.15376/biores.16.2.2953-2970

Nabora CS, Kingondu CK, Kivevele TT (2019) *Tamarindus indica* fruit shell ash: a low cost and effective catalyst for biodiesel production from *Parinari curatellifolia* seeds oil. SN Appl Sci 1:1–9. https://doi.org/10.1007/s42452-019-0256-3

Nawaz MA, Zakharenko AM, Zemchenko IV et al (2019) Phytolith formation in plants: from soil to cell. Plants 8:249. https://doi.org/10.3390/plants8080249

Ndjamba A, Pérez Y, Cárdenas V et al (2021) Modelos De Regressão para Estimativa do volume de Fuste E Ramos Da Espécie *Brachystegia Gossweilerii* Hutch. & Burt Davy, na Floresta do Miombo Da Comuna do Cuima (Huambo-Angola). (regression models for estimating the volume of stem and branches of the species *Brachystegia Gossweilerii* Hutch. & Burt Davy, in the Miombo Forest of the commune of Cuima (Huambo-Angola)). Silva Lusit 29:53–71. https://doi.org/10.1051/silu/20212901053

Neiva DM, Araújo S, Gominho J et al (2018) An integrated characterization of *Picea abies* industrial bark regarding chemical composition, thermal properties and polar extracts activity. PLoS ONE 13:1–14. https://doi.org/10.1371/journal.pone.0208270

Ogunbolude Y, Ajayi MA, Ajagbawa TM et al (2009) Ethanolic extracts of seeds of *Parinari curatellifolia* exhibit potent antioxidant properties: a possible mechanism of its antidiabetic action. J Pharmacognosy Phytotherapy 1:67–075

Omale S, Aguiyi JC, Adekunle OG et al (2020) Evaluation of the Antidiabetic effects of the Stem Bark Extract of *Parinari Curatellifolia* (Planch. Ex Benth.) In *Drosophila melanogaster*. J Pharmacol Toxicol 16:9–21. https://doi.org/10.3923/jpt.2021.9.21

Orwa C, Mutua A, Kindt R et al (2009) Agroforestree Database: a tree reference and selection guide version 4.0. https://apps.worldagroforestry.org/treedb2/speciesprofile.php?Spid=1253. Accessed 4 Aug 2023

Palgrave MC (2002) Trees of Southern Africa, Randomstru. Struik Nature, Cape Town

Parameswaran N, Liese W (1974) Variation of cell length in bark and wood of tropical trees. Wood Sci Technol 8:81–90. https://doi.org/10.1007/BF00351364

Peni IJ, Elinge CM, Yusuf H et al (2010) Phytochemical screening and antibacterial activity of *Parinari curatellifolia* stem extract. J Med Plants Res 4:2099–2102

Petit G, Crivellaro A (2014) Comparative axial widening of phloem and xylem conduits in small woody plants. Trees - Struct Function 28:915–921. https://doi.org/10.1007/s00468-014-1006-1

Prance GT (2007) Flora da Reserva Ducke, Amazonas, Brasil: Chrysobalanaceae. (Flora of the Ducke Reserve, Amazon, Brazil: Chrysobalanaceae). Rodriguésia 58:493–531

Quilhó T, Pereira H, Richter HG (2000) Within-tree variation in phloem cell dimensions and proportions in *Eucalyptus globulus*. IAWA J 21:31–40. https://doi.org/10.1163/22941932-90000234

Quilhó T, Sousa V, Tavares F, Pereira H (2013) Bark anatomy and cell size variation in *Quercus faginea*. Turk J Bot 37:561–570. https://doi.org/10.3906/bot-1201-54

Ralph J, Hatfield D, Hatfield R RD (1991) Pyrolysis-GC-MS characterization of forage materials. J Agric Food Chem 39:1426–1437. https://doi.org/10.1021/jf00008a014

Richter HG, Dallwitz MJ (2000) Commercial timbers: descriptions, illustrations, identification, and information retrieval. https://www.delta-intkey.com/wood/index.htm. Accessed 4 Aug 2023

Roth I (1981) Structural patterns of tropical barks. Borntraeger, Berlim

Sánchez-Moreno C, Larrauri JA, Saura-Calixto F (1998) A procedure to measure the antiradical efficiency of polyphenols. J Sci Food Agric 76:270–276. https://doi.org/10.1002/(SICI)1097-0010(199802)76:2%3C270::AID-JSFA945%3E3.0.CO;2-9

Sanfilippo M (2014) Trinta árvores do miombo Angolano. Guia De campo para a identificação. (thirty Angolan miombo trees. Field Guide for Identification). COSPE, Firenze

Sangumbe LMV, Pereira M, Carrillo I, Mendonça RT (2018) An exploratory evaluation of the pulpability of *Brachystegia spiciformis* and *Pericopsis angolensis* from the angolan miombo woodlands. Maderas Ciencia y tecnología 20:0–0. https://doi.org/10.4067/S0718-221X2018005002301

Schweingruber FH (2007) Wood structure and environment. Springer-Verlag GmbH, Germany

Şen A, Quilhó T, Pereira H (2011) The cellular structure of cork from *Quercus cerris* var. Cerris bark in a materials' perspective. Ind Crops Prod 34:929–936. https://doi.org/10.1016/j.indcrop.2011.02.015

Shoko T, Saka JDK, Apostolides Z (2014) Headspace volatiles of the edible fruit pulp of *Parinari Curatellifolia* growing in Malawi using solid phase microextraction. South Afr J Bot 90:128–130. https://doi.org/10.1016/j.sajb.2013.11.001

Sousa V, Ferreira JPA, Miranda I et al (2021) *Quercus Rotundifolia* Bark as a source of Polar extracts: structural and chemical characterization. Forests 12:1160. https://doi.org/10.3390/f12091160

TAPPI (1991) TAPPI UM 250. Acid-soluble lignin in Wood and Pulp. TAPPI, Atlanta

TAPPI (2002a) T 258 om-02. Basic density and moisture content of pulpwood. TAPPI, Atlanta

TAPPI (2007a) T 211 om-93. Ash in wood, pulp, paper and paperboard: combustion at 525°C. TAPPI, Atlanta

TAPPI (2007b) T 204 Cm-97. Solvent extractives of wood and pulp. TAPPI, Atlanta

TAPPI (2002b) T 222 om-02. Acid-insoluble lignin in wood and pulp. Atlanta

Ter Welle BJH (1975) Spiral thickenings in the Axial Parenchyma of Chrysobalanaceae*. Acta Bot Neerlandica 24:397–405. https://doi.org/10.1111/j.1438-8677.1975.tb01030.x

Vangeel T, Neiva DM, Quilhó T et al (2021) Tree bark characterization envisioning an integrated use in a biorefinery. https://doi.org/10.1007/s13399-021-01362-8. Biomass Convers Biorefin 2029–2043

Zobel BJ, van Buijtenen JP (1989) Wood Variation and Wood properties. Wood Variation. Springer Series in Wood Science, Berlin, pp 1–32

Publisher's Note Springer Nature remains neutral with regard to jurisdictional claims in published maps and institutional affiliations.